# Immersed boundary methods for numerical simulation of confined fluid and plasma turbulence in complex geometries


***Kai Schneider***

*Aix-Marseille Université, France*


*7th ITER International School*

High Performance Computing in Fusion Science

August 25th – 29th, 2014, Aix-en-Provence, France

# Acknowledgements


- Philippe Angot (Marseille)
- Wouter Bos (Lyon)
- Thomas Engels (Berlin/Marseille)
- Marie Farge (Paris)
- Benjamin Kadoch (Marseille)
- Dmitry Kolomenskiy (Montreal)
- Matthieu Leroy (Marseille)
- David Montgomery (Dartmouth)
- Jorge Morales (Lyon/Cadarache)
- Salah Neffaa (Marseille)
- Romain Nguyen van yen (Toulouse)

# Outline

- Motivation
- The volume penalization method for fixed (~~and moving~~) obstacles
- Analysis of the penalized Laplace operator
  - 1d example for Dirichlet and Neumann boundary conditions
- Applications to fluid turbulence (Navier-Stokes eq.) :
  - 2d confined turbulence, flapping wings in 3d
  - Application to passive scalars (turbulent mixing)
- Applications to plasma turbulence (Navier-Stokes + Maxwell eq.)
  - Spontanuous rotation in toroidally confined MHD
  - Effect of toroidicity in RFP dynamics
- Conclusions

# Context: Immersed boundary methods

cartesian geometry

spectral/wavelet solvers
for Navier-Stokes equ.

+

complex geometry

???

=

penalty approach

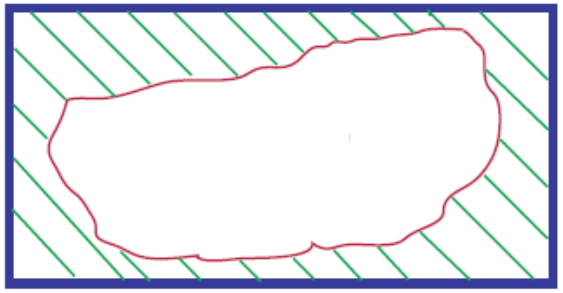

use solver in cartesian
geometry
+ penality term

Different strategies:
- surface penalisation, Peskin, '70ies
- volume penalisation, Caltagirone, '80ies
- imbedding methods, Glowinski, '80ies

# Physically motivated mathematical model

- **Solid moving wings**
- **Viscous incompressible fluid**

$$\partial_t \mathbf{u} + \mathbf{u}\cdot\nabla\mathbf{u} + \frac{1}{\rho}\nabla p - \nu\nabla^2\mathbf{u} = 0,$$
$$\nabla\cdot\mathbf{u} = 0,$$

$$\mathbf{u}|_{\partial\Omega} = \mathbf{u}_s|_{\partial\Omega}$$

$$A = A_f \cup A_s$$

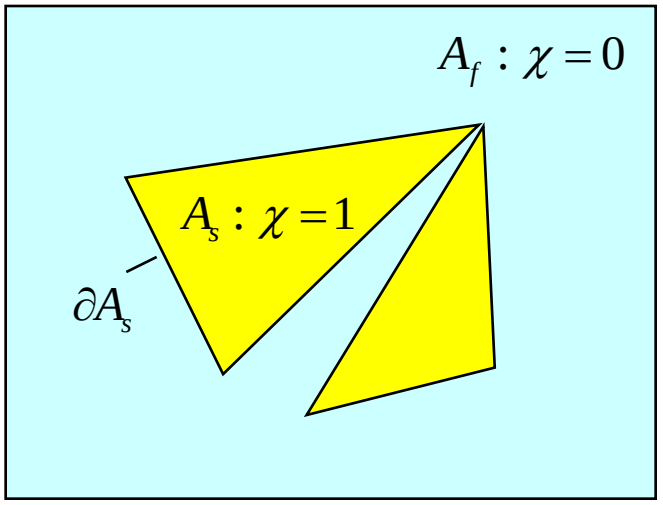


**Penalized equation:**

$$\partial_t \mathbf{u}_\eta + \mathbf{u}_\eta\cdot\nabla\mathbf{u}_\eta + \frac{1}{\rho}\nabla p_\eta - \nu\nabla^2\mathbf{u}_\eta + \frac{\chi}{\eta}(\mathbf{u}_\eta - \mathbf{u}_s) = 0$$

**Volume penalization method is physically motivated**

E. Arquis and J.P. Caltagirone, 1984.
*C. R. Acad. Sci. Paris*, **II**

- **Mathematically justified**

P. Angot, C.H. Bruneau and P. Fabrie, 1999.
*Numer. Math.* **81**

G. Carbou and P. Fabrie, 2003.
*Adv. Diff. Equations* **8**

- **Easy-to-implement**

K. Schneider, 2005. *Comput. Fluids* **34**

Hydrodynamic force

$$\mathbf{F}/\rho = \int_A \frac{\chi}{\eta}(\mathbf{u}_\eta - \mathbf{u}_s)dA + V_c\frac{d\mathbf{u}_c}{dt}$$

$\mathbf{u}_s$ – pointwise velocity of the solid
$\mathbf{u}_c$ – velocity of the center of the solid
$V_c$ – volume of the solid

# Initial Boundary Value Problem In complex geometry

$$Lu = f \quad \text{for} \quad \boldsymbol{x} \in \Omega_f$$

with $bu = g$ at $\partial\Omega_f$ (Plus initial conditions)

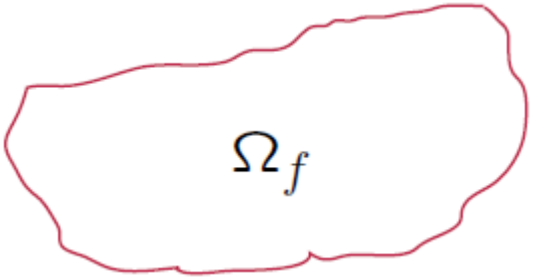


with *L* being, e.g. the Laplace operator, or Navier-Stokes or Maxwell operator

# Penalized problem in simple geometry

$$Lu_\eta = f - \frac{1}{\eta}\chi(bu - g) \quad \text{for} \quad \boldsymbol{x} \in \Omega = \Omega_f \cup \Omega_s$$

Penalization (modeling) error: $\| u - u_\eta \| \propto \eta^\alpha$

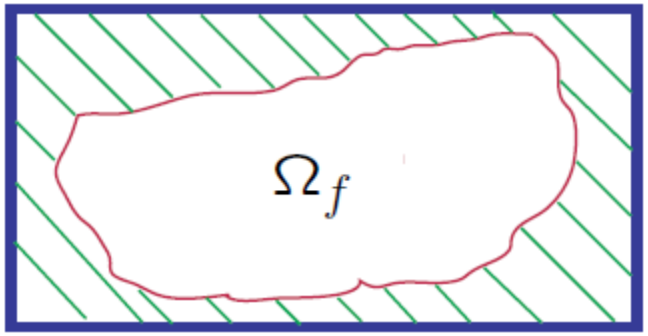

# Discretized penalized problem

$$L^N u_\eta^N = f^N - \frac{1}{\eta}\chi^N(bu - g) \quad \text{for} \quad \boldsymbol{x} \in \Omega$$

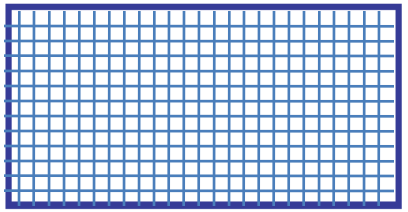

with $\triangle x \propto 1/N$

Discretization error: $\| u_\eta - u_\eta^N \| \propto \left(\frac{1}{N}\right)^\beta$

Total error = modeling error + discretization error

$$\| u - u_\eta^N \| \leq \| u - u_\eta \| + \| u_\eta - u_\eta^N \|$$

# Some analysis: a simple example

Let us consider the one-dimensional Poisson equation

$$-\frac{\mathrm{d}^2 w(x)}{\mathrm{d}x^2} = f(x)$$

with $x \in \Omega = ]0, \pi[$, homogeneous Dirichlet boundary conditions

$$w(0) = 0, \quad w(\pi) = 0$$

and the right-hand side given by a sinusoidal function

$$f(x) = m^2 \sin mx.$$

The exact solution to this problem is

$$w(x) = \sin mx.$$

# Exact solution of the penalized 1d Poisson equation

Let us now solve this problem approximately using the volume penalization method. The domain is extended to $\mathbb{T} = \mathbb{R}/2\pi\mathbb{Z}$. The Poisson equation is modified by adding the penalization term,

Penalization term

$$-v'' + \frac{1}{\eta}\chi v = f, \tag{5}$$

where $''$ denotes the second derivative with respect to $x$, $f$ is extended naturally through $\mathbb{T}$ using the original formula (3) and the mask function is

$$\chi = \begin{cases} 0, & x \in ]0, \pi[ \\ 1/2, & x = 0,\ x = \pi \\ 1, & x \in ]\pi, 2\pi[ \end{cases} \tag{6}$$

Periodic boundary conditions are imposed at $x = 0$ and $x = 2\pi$. The exact solution to the penalized problem is

$$v(x) = \begin{cases} \sin mx + A_1 x + A_2, & x \in [0, \pi[ \\ \frac{m^2\eta}{1+\eta m^2} \sin mx + B_1 e^{-x/\sqrt{\eta}} + B_2 e^{x/\sqrt{\eta}}, & x \in [\pi, 2\pi[ \end{cases} \tag{7}$$

# Exact solution of the penalized 1d Poisson equation (3)

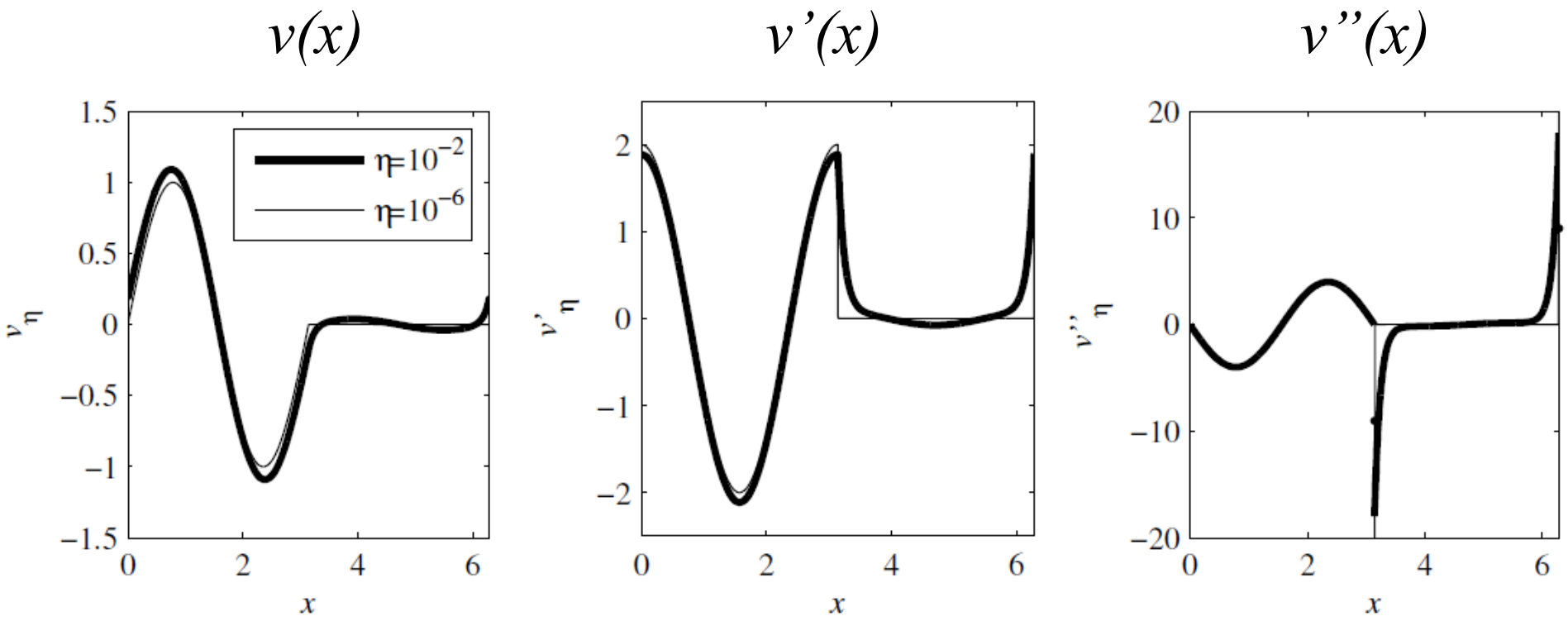


Exact penalized solution (left) for $m$=2 and its first (center) and second (right) derivatives.

# Penalization error of the Dirichlet problem

Using the exact solution of the penalized problem the leading order $L^2$ error with respect to the Dirichlet problem is given by

$$\varepsilon_1 \sim \frac{m\sqrt{2-(-1)^m}}{\sqrt{6}}\sqrt{\eta} \quad \text{as} \quad \eta \to 0$$

where the $\sqrt{\eta}$ behavior is consistent with previous studies by Angot et al., 1999 and Carbou and Fabrie, 2003.

# Discretization error of the penalized equation

The penalized problem is discretized with a pseudospectral Fourier method using $N$ grid points. For the $L^2$ error between the discrete solution and the exact solution of the penalized problem we get,

$$\varepsilon_2 \sim K \frac{m\pi^{3/2}}{3\sqrt{2}} \frac{1}{\sqrt{\eta} N^2} \quad \text{as} \quad \eta \to 0, \quad \sqrt{\eta} N^2 \to \infty,$$

where $K$=2 for $m$ even and $K \approx 3.84$ for $m$ odd.
The $N^{-2}$ behavior is related to the regularity the exact penalized solution as observed by Min & Gottlieb 2003 for elliptic equations with discontinuous coefficients.

# How to choose η?

Combining the two estimates we get a bound for the total error $\varepsilon$ between the discrete-penalized solution and the exact solution of the Dirichlet problem:

$$\varepsilon \leq \varepsilon_1 + \varepsilon_2 \sim \frac{m\sqrt{2-(-1)^m}}{\sqrt{6}}\sqrt{\eta} + K\frac{m\pi^{3/2}}{3\sqrt{2}}\frac{1}{\sqrt{\eta}N^2} \quad \text{as} \quad \eta \to 0, \quad \sqrt{\eta}N^2 \to \infty$$

When η is chosen with the right order of magnitude, i.e. $\eta \propto 1/N$, in order to optimize the preceding estimate, then the resulting error is

$$\varepsilon \propto \frac{1}{N}$$

which suggests that the penalization method with Fourier discretization is a first order method.

# Convergence of the Fourier collocation method

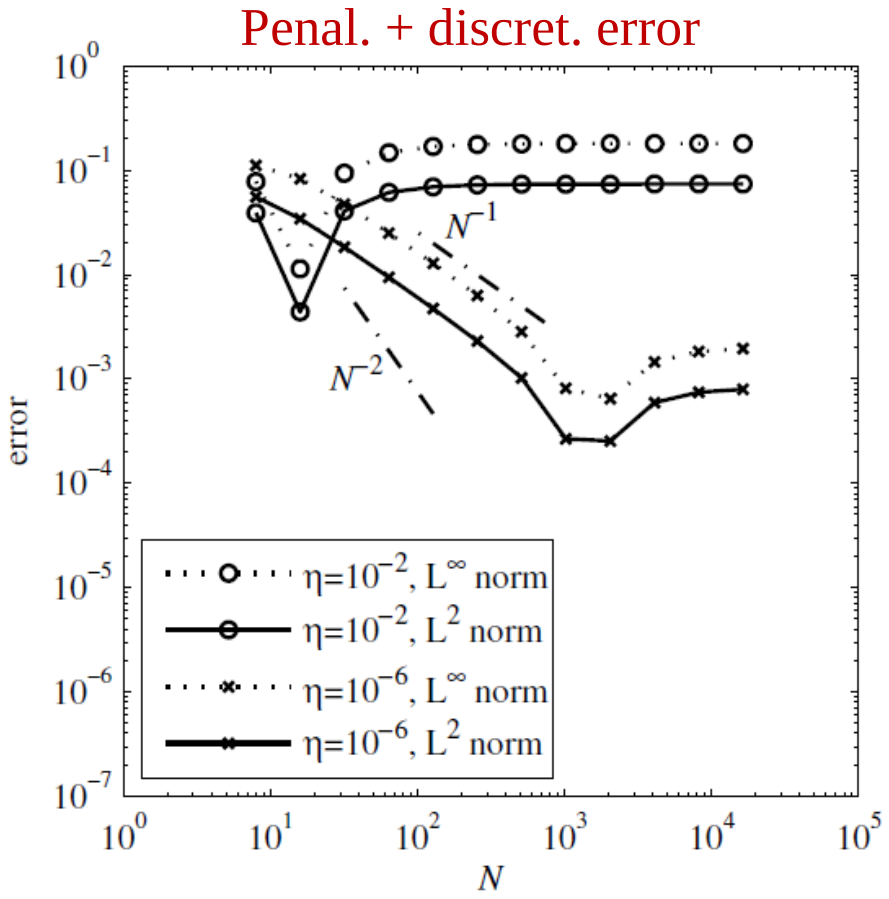


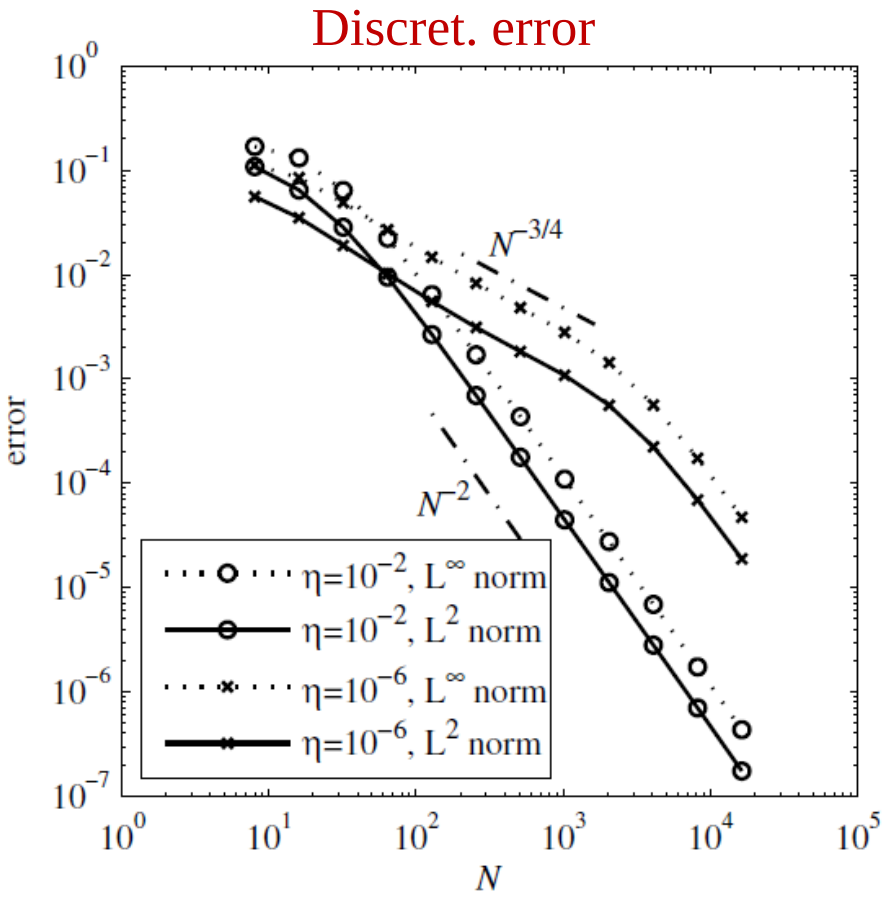


Error with respect to the exact Dirichlet solution in the interior of the fluid domain (left) and with respect to the penalized solution in the whole domain (right).

# The volume penalization method for fixed (~~and moving~~) obstacles

# Navier-Stokes equations

# Two- and three-dimensional formulations

**Two-dimensional model:**

$$\partial_t \omega_\eta + \mathbf{u}_\eta \cdot \nabla \omega_\eta - \nu \nabla^2 \omega_\eta + \nabla \times \left( \frac{\chi}{\eta} (\mathbf{u}_\eta - \mathbf{u}_s) \right) = 0$$

$$\nabla^2 \Psi_\eta = \omega_\eta$$

$$\mathbf{u}_\eta = \nabla^\perp \Psi_\eta + \mathbf{U}_\infty$$

$$\omega_\eta = \nabla \times \mathbf{u}_\eta$$

**Three-dimensional model:**

$$\partial_t \mathbf{u}_\eta + \boldsymbol{\omega}_\eta \times \mathbf{u}_\eta + \nabla \Pi_\eta - \nu \nabla^2 \mathbf{u}_\eta + \frac{\chi}{\eta} (\mathbf{u}_\eta - \mathbf{u}_s) = 0$$

$$-\nabla^2 \Pi_\eta = \nabla \cdot (\boldsymbol{\omega}_\eta \times \mathbf{u}_\eta + \frac{\chi}{\eta} (\mathbf{u}_\eta - \mathbf{u}_s)) = 0$$

$$\Pi_\eta = p_\eta + u_\eta^2 / 2$$

$$\boldsymbol{\omega}_\eta = \nabla \times \mathbf{u}_\eta$$

# Numerical method

• Pseudo-spectral Fourier discretization in space (periodic boundary conditions)
**Fast Fourier Transform**

• Exact integration of the viscous term (method of integrating factors)

$$\partial_t \hat{\omega}_\eta + \nu |\mathbf{k}|^2 \hat{\omega}_\eta = \hat{N}(\hat{\omega}_\eta)$$

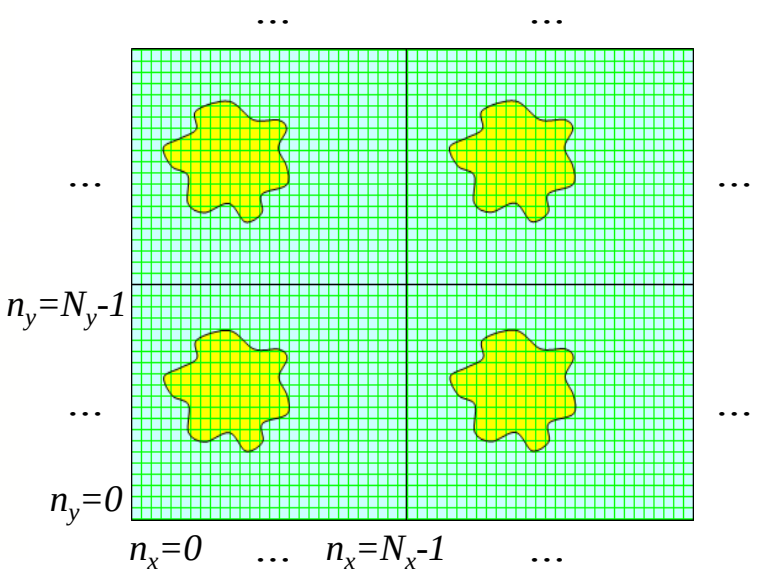


• Adaptive 2nd order Adams-Bashforth time-stepping scheme


Ref.: K. Schneider, 2005. *Comput. Fluids* **34**
D. Kolomenskiy and K. Schneider, 2009. *J. Comput. Phys.* **228**

# Application to

# 2d confined turbulence

# 2D decaying turbulence in a circular domain

Mask:

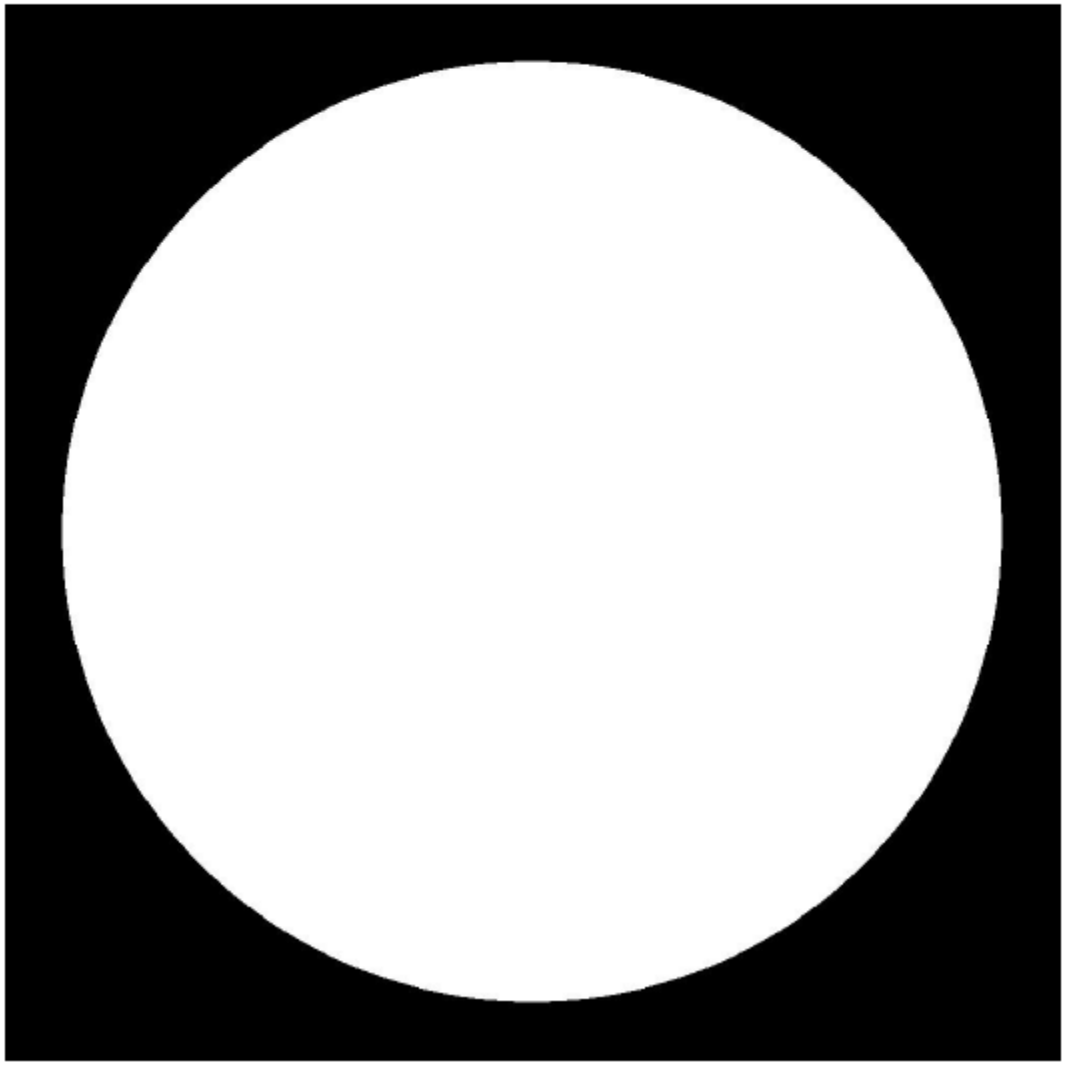

# 2d decaying turbulence in a circular domain

Vorticity,
$N=1024^2$

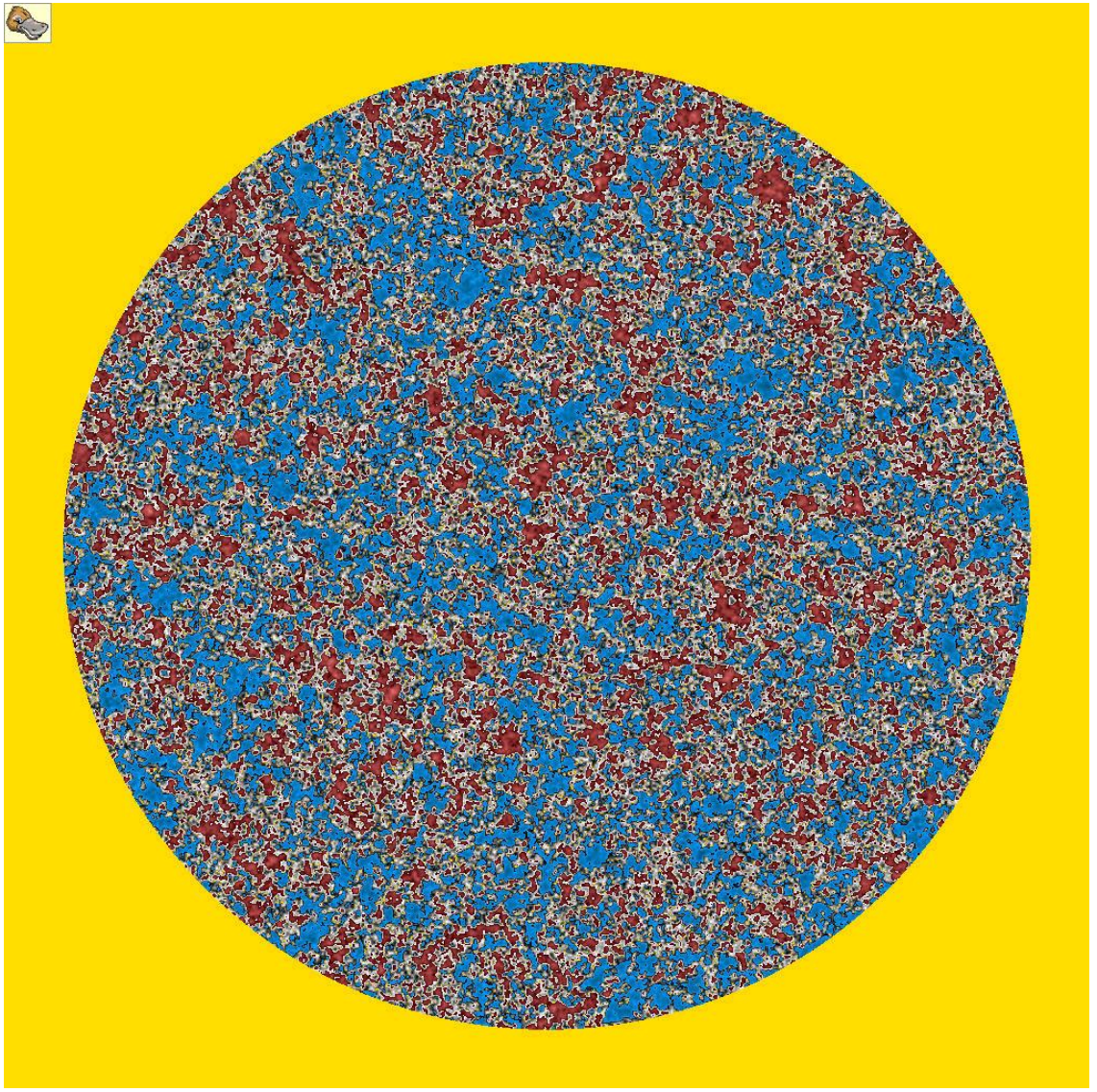

C:\Users\kschneid\
cuments\TALK_INI_2



Ref.: K. Schneider and M. Farge, *Phys. Rev. Lett.*, 95(24), 2005

# 2D decaying turbulence in a circular domain

Streamfunction:
t=320

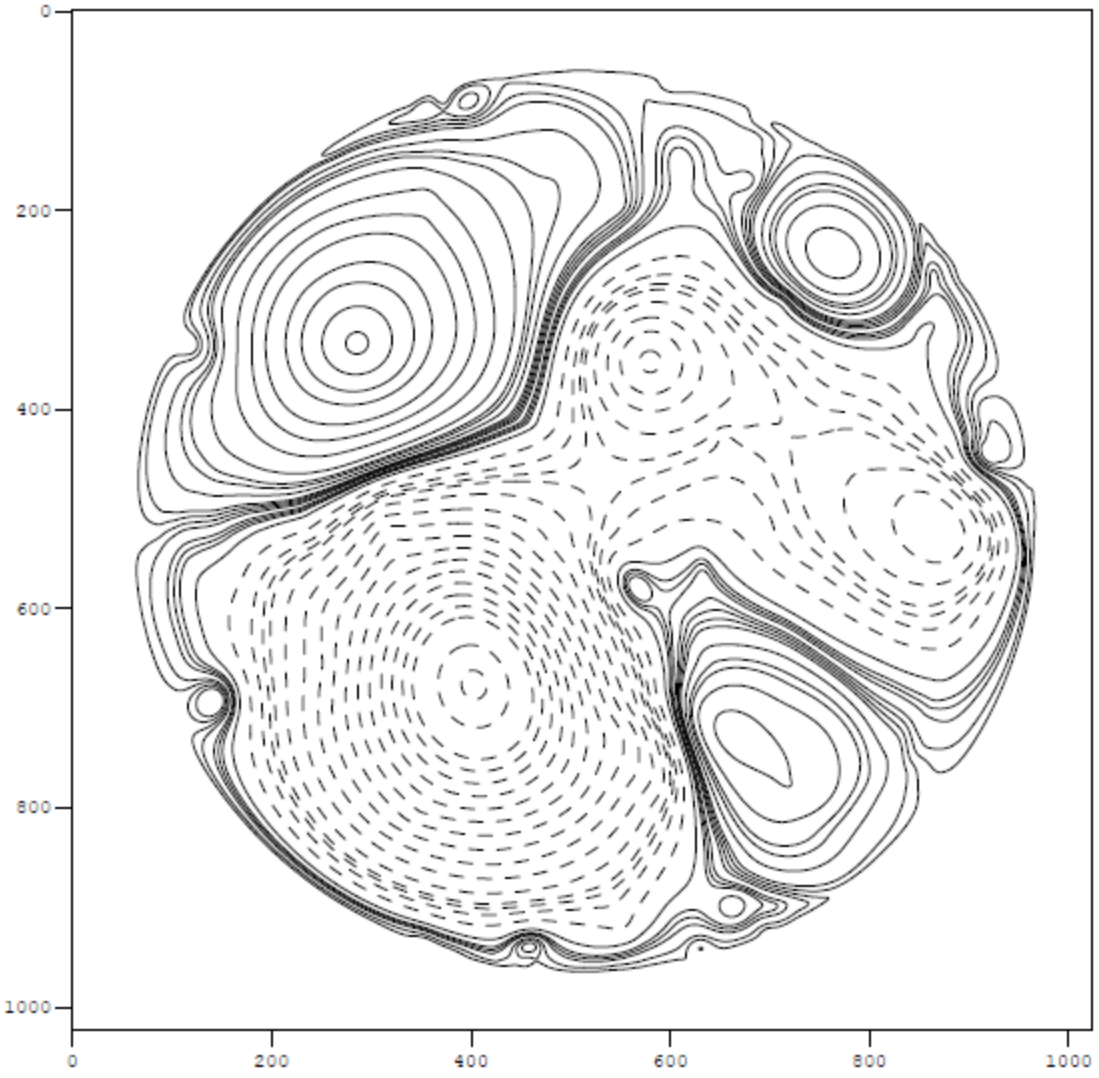

# 2D decaying turbulence in a circular domain

## Cuts at t=320

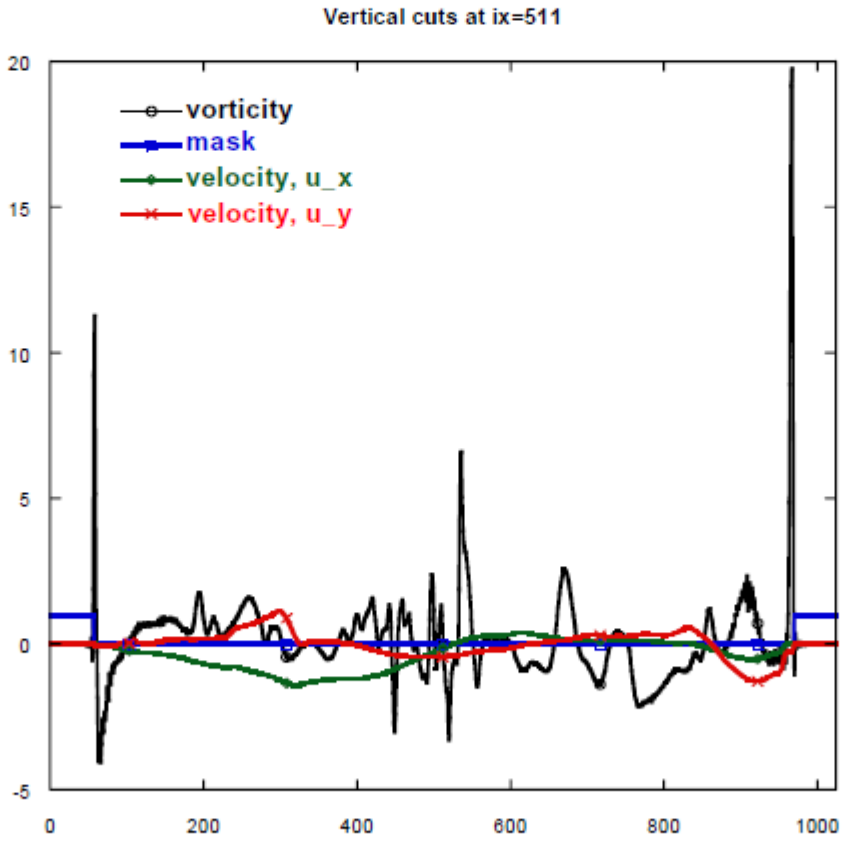


Vertical cuts of vorticity, and the velocity components together with the mask function

# 2D decaying turbulence in a circular domain

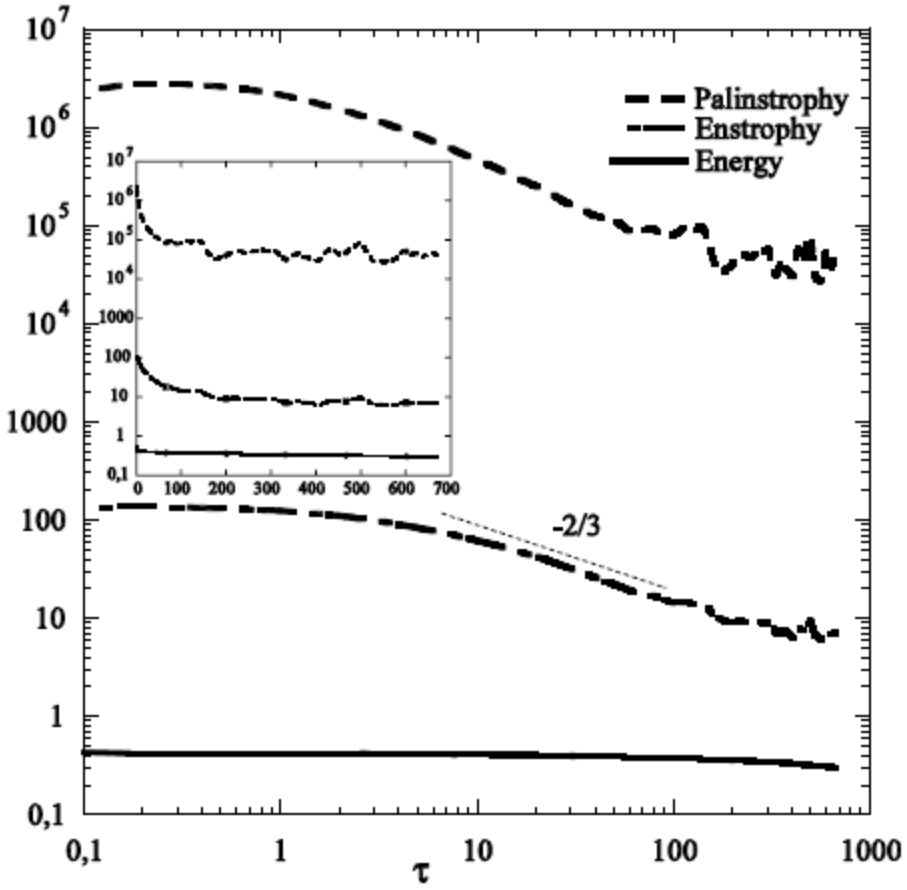


Time evolution of energy E, enstrophy Z and palinstrophy P.

# 2D decaying turbulence in a circular domain

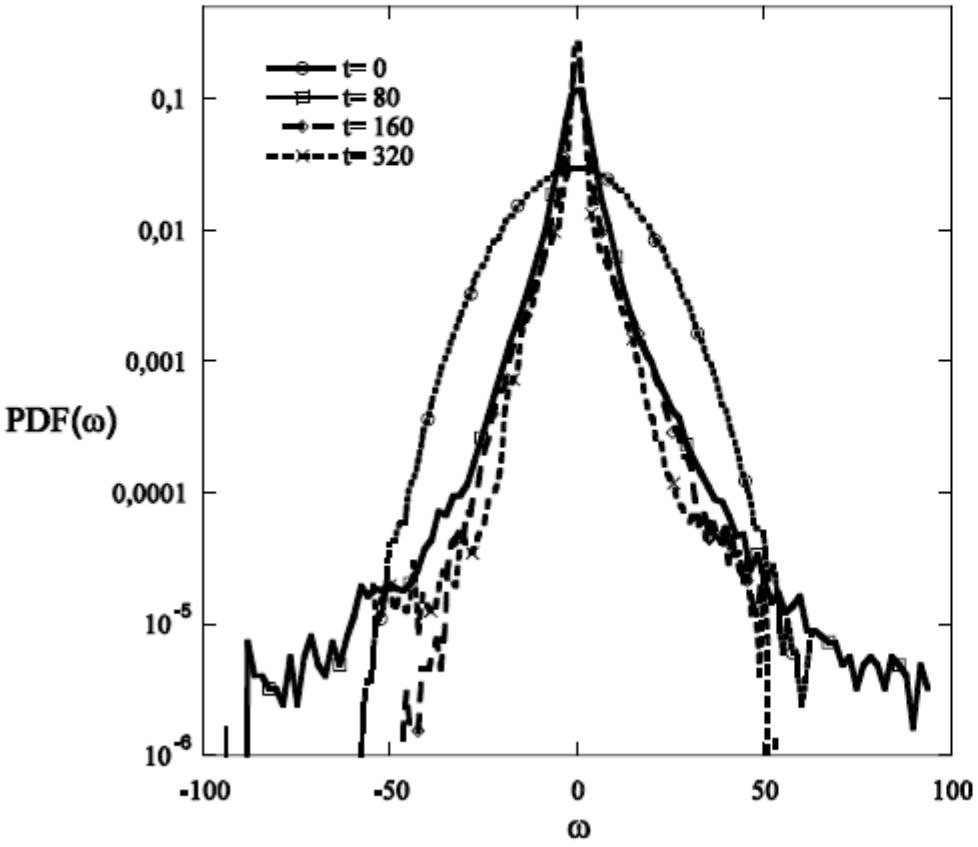


PDF of vorticity ω.

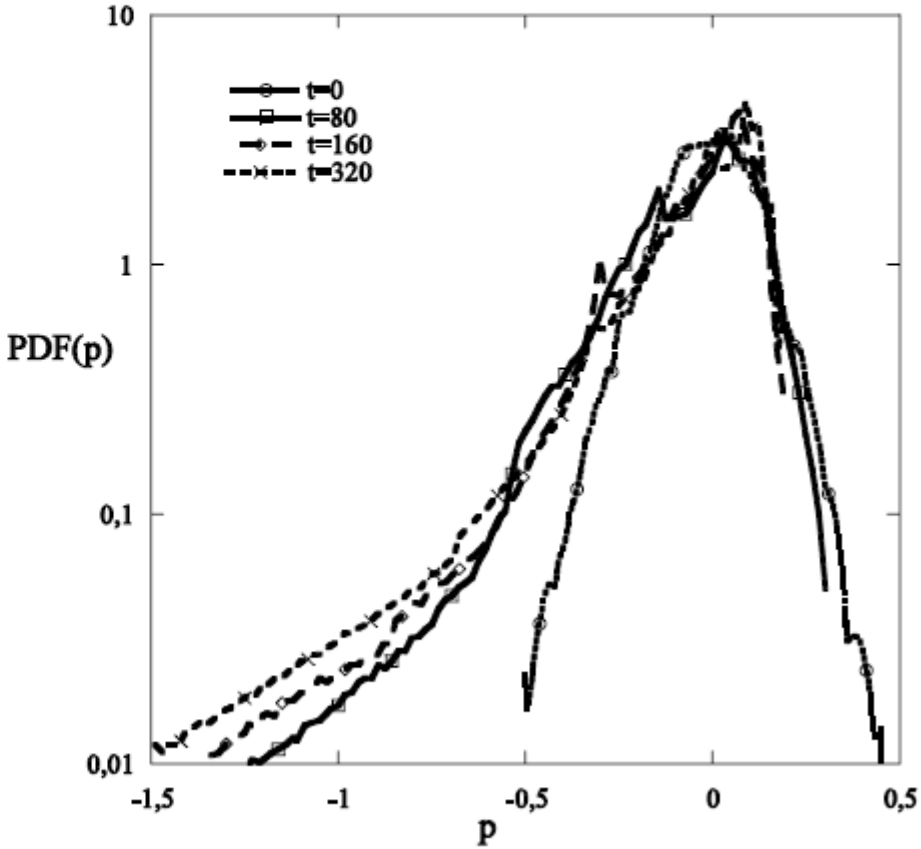


PDF of pressure p.

# Flapping wings:‘Realistic’ planform and kinematics

www.vapor.ucar.edu



Ref.: D. Kolomenskiy, H.K. Moffatt, M. Farge, K. Schneider. *J. Fluids Struc.*, 2011

# Penalization for Fluid structure interaction: flexible beam

Configuration:

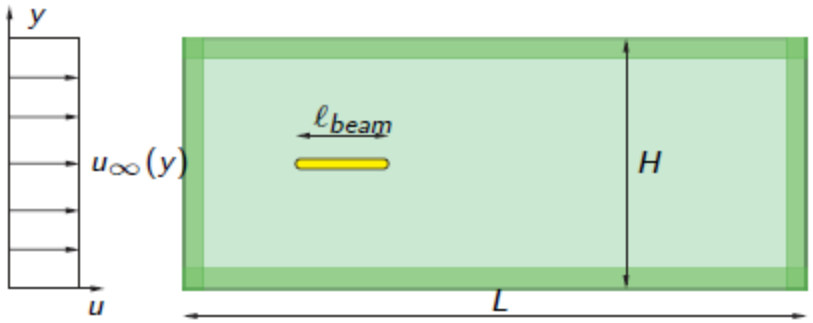


Simulations at $\mathrm{Re} \to \infty$ and linear stability analysis predict three regimes: stable, periodic, chaotic.

We investigate the influence of the Reynolds number and choose $\mathrm{Re} = 20, 100, 200$.

# Vorticity, Re=200, $\eta=10^{-3}$ (chaotic state)



Ref.: Th. Engels, D. Kolomenskiy, K. Schneider and J. Sesterhenn, *Comput. & Struc*. 122, 2013.

# ‘Swimming’ flapping flexible foil


swimmer_three_perspectives.avi

# ‘Insect flight’


insect_rigid_turb.avi

Simulations by Thomas Engels.

# Neumann boundary conditions (I)

As simple example we consider the Poisson equation,

$$-w'' = f \quad \text{for} \quad x \in (0, \pi)$$

with homogeneous Neumann boundary conditions

$$w'(x = 0) = w'(x = \pi) = 0$$

and for $f(x) = m^2 \cos mx,\ m \in \mathbb{Z}$

The exact solution is $w(x) = \cos mx + C$ where $C$ is a constant.

The penalized equation reads

$$-d_x(1 - \chi) + \eta\chi)d_x v = f \quad \text{for} \quad x \in (0, 2\pi)$$

with the penalization parameter η is and the mask function

$$\chi(x) = \begin{cases} 0 & \text{for} \quad 0 < x < \pi \\ 1/2 & \text{for} \quad x = 0 \text{ or } x = \pi \\ 1 & \text{elsewhere} \end{cases}$$

Periodic boundary conditions are imposed.

# Neumann boundary conditions (II)

The exact solution of the penalized problem is

$$v(x) = \begin{cases} \cos mx + A_1 x + A_2 & \text{for} \quad x \in ]0, \pi[ \\ B_1 x + B_2 & \text{for} \quad x \in ]\pi, 2\pi[ \end{cases}$$

where 3 of the 4 coefficients can be determined by imposing continuity of the solution and of the flux.

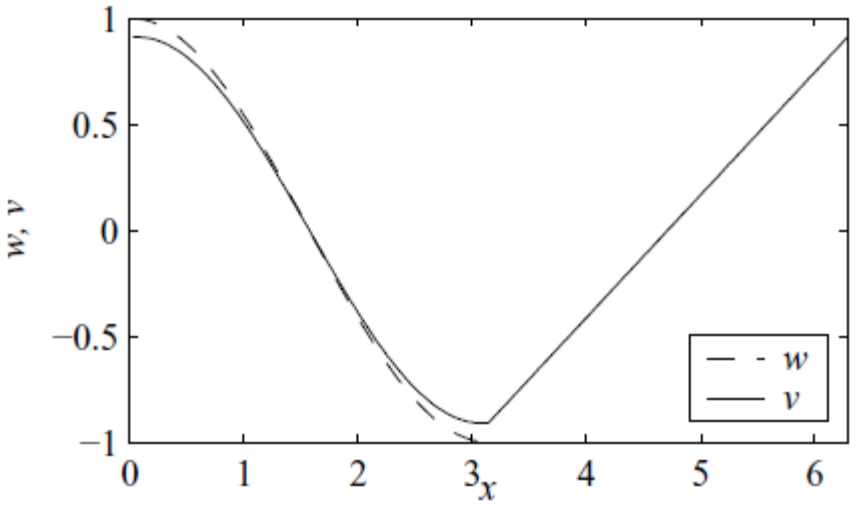


Figure 1: $w(x)$ and $v(x)$ for $m = 1$.

The Fourier coefficients of v decay like $k^{-2}$ and there is no boundary layer!

For details:

D. Kolomenskiy, R. Nguyen van yen, K.S., arXiv:1403.5948, *Applied Numerical Mathematics*, in press, 2014

# Neumann boundary conditions (III)

Advection-diffusion equation of a passive scalar,

$$\frac{\partial \theta}{\partial t} + ((1-\chi)\boldsymbol{u}) \cdot \nabla\theta = \nabla \cdot ([\kappa(1-\chi) + \eta_\theta \chi]\nabla\theta)$$

where $\theta$ is the passive scalar, $\kappa$ is the diffusivity and $\eta_\theta$ is the penalization parameter.

The penalization term models the no-flux boundary condition at the wall $\nabla\theta \cdot \boldsymbol{n}|_{\Omega_f} = 0$

The numerical method is a Fourier pseudo-spectral method, resolution $1024^2$.

Ref.: B. Kadoch, D. Kolomenskiy, P. Angot, and K. Schneider, *J. Comput. Phys.*, 231, 2012

# Passive scalar mixing

B. Kadoch, D. Kolomenskiy, P. Angot, K. Schneider, *JCP*, 231, 2012

## Vorticity

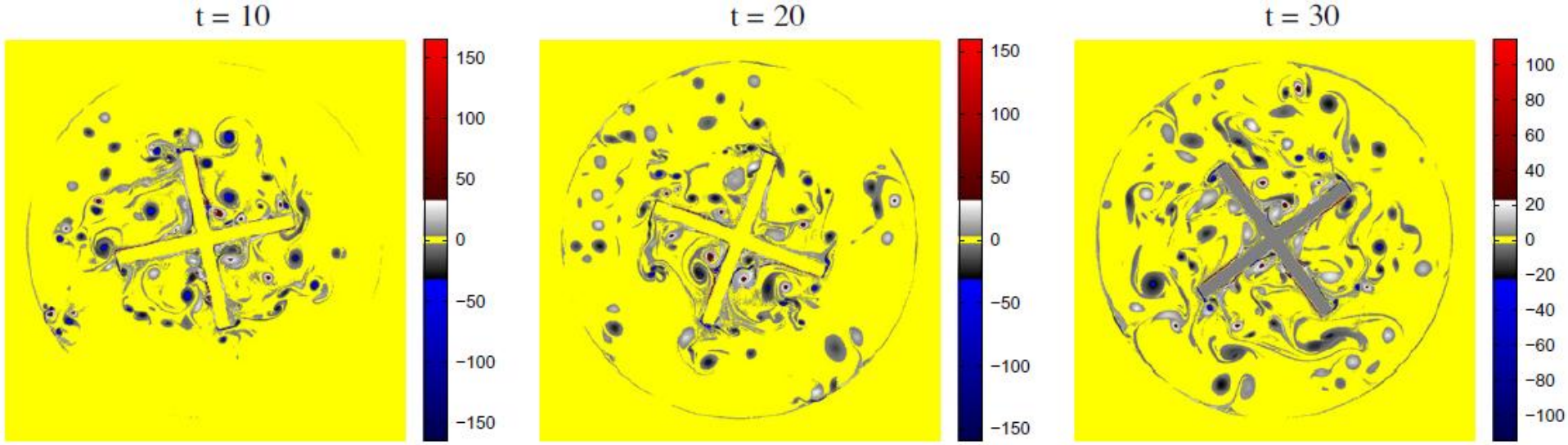


## Scalar field

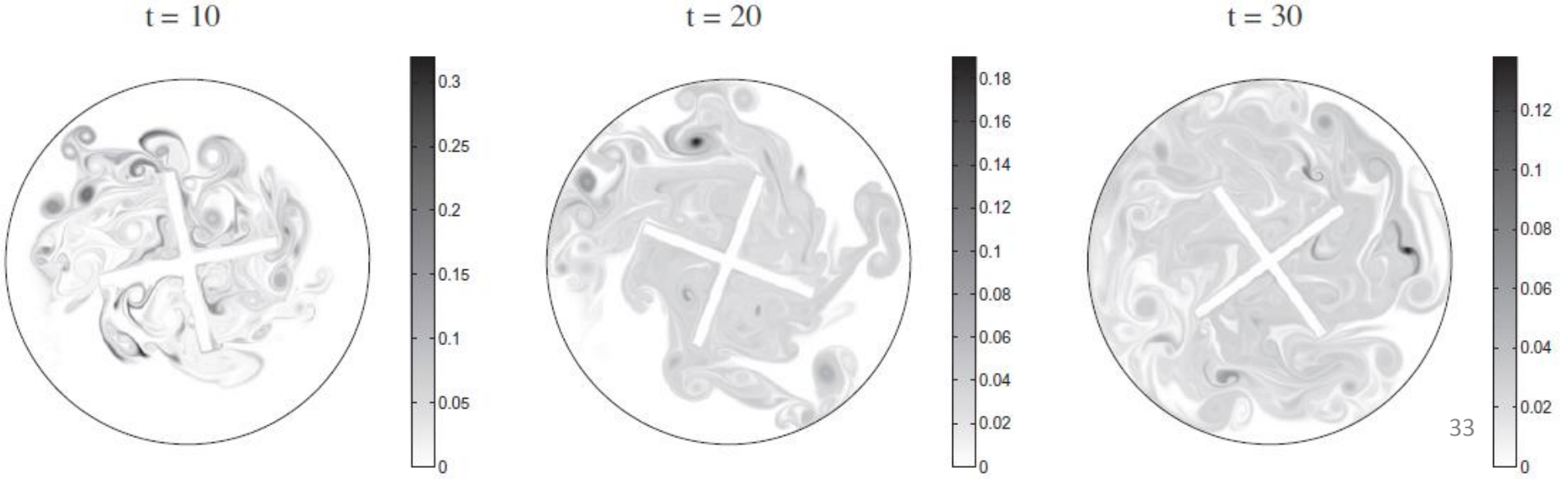

# The volume penalization method for MHD equations

# Application to

## Spontanuous rotation in toroidally confined MHD

Ref.: J. Morales, W. Bos, K. Schneider and D. Montgomery, *Phys. Rev. Lett.*, **109** , 2012.

# Introduction

- A good plasma confinement is essential to increase the performances of a fusion reactor.
- Turbulent fluctuations $\longrightarrow$ reduction of the confinement.
- Under certain conditions turbulence is reduced $\longrightarrow$ **L-H transition**.
- **Toroidal rotation?** Is either at the origin or a consequence of this mechanism (Rice *et al.*, Nucl. Fusion, 2007).

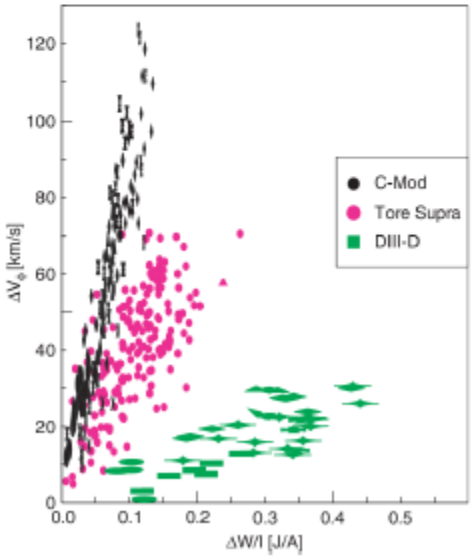

# A magnetohydrodynamic (MHD) description

MHD description → the plasma is described as a charge-neutral conducting fluid. The dimensionless incompressible MHD equations for the velocity $\boldsymbol{u}$ and magnetic field $\boldsymbol{B}$,

$$\frac{\partial \boldsymbol{u}}{\partial t} - \frac{1}{M}\nabla^2 \boldsymbol{u} = -\nabla\left(P + \frac{1}{2}\boldsymbol{u}^2\right) + \boldsymbol{u}\times\omega + \boldsymbol{j}\times\boldsymbol{B}, \qquad (1)$$

$$\frac{\partial \boldsymbol{B}}{\partial t} = -\nabla\times\boldsymbol{E}, \qquad \boldsymbol{E} = \frac{1}{S}\boldsymbol{j} - \boldsymbol{u}\times\boldsymbol{B}, \qquad (2)$$

$$\nabla\cdot\boldsymbol{u} = 0, \qquad \nabla\cdot\boldsymbol{B} = 0, \qquad (3)$$

with current density $\boldsymbol{j} = \nabla\times\boldsymbol{B}$, vorticity $\omega = \nabla\times\boldsymbol{u}$, pressure $P$ and electric field $\boldsymbol{E}$.

**Dynamics are governed by,**

$$M = \frac{C_A L}{\nu}, \quad S = \frac{C_A L}{\lambda}, \quad \text{Boundary \& Initial conditions.} \qquad (4)$$

# Background

- Montgomery & Shan (1994) and Bates & Lewis (1996) investigated the case of viscoresistive MHD in a toroidal geometry.
- In the case of uniform resistivity and imposed curl-free toroidal electric and magnetic fields, **no static equilibria → dynamic equilibria.**

$$\nabla \times (\boldsymbol{j} \times \boldsymbol{B}) \neq 0 \implies \nabla P \neq \boldsymbol{j} \times \boldsymbol{B} \implies \boldsymbol{u} \neq 0. \qquad (5)$$

- Hence **vorticity is created**.

$$\frac{\partial \omega}{\partial t} - M^{-1}\nabla^2 \omega - \nabla \times (\boldsymbol{u} \times \omega) = \nabla \times (\boldsymbol{j} \times \boldsymbol{B}) \neq 0. \qquad (6)$$

- It is necessary to take into account **all other terms** in the MHD equations.
- To study the full dynamics the equations are solved numerically.

# Numerical simulations

- Curl-free toroidal magnetic and electric fields are considered,

$$\mathbf{B}_{\theta_{ext}}(R) = B_0 \frac{R_0}{R} \boldsymbol{e}_\theta, \qquad \mathbf{J}_{\theta_{ext}}(R) = J_0 \frac{R_0}{R} \boldsymbol{e}_\theta. \tag{7}$$

- The safety factor at the edge is fixed, $q = 3$.

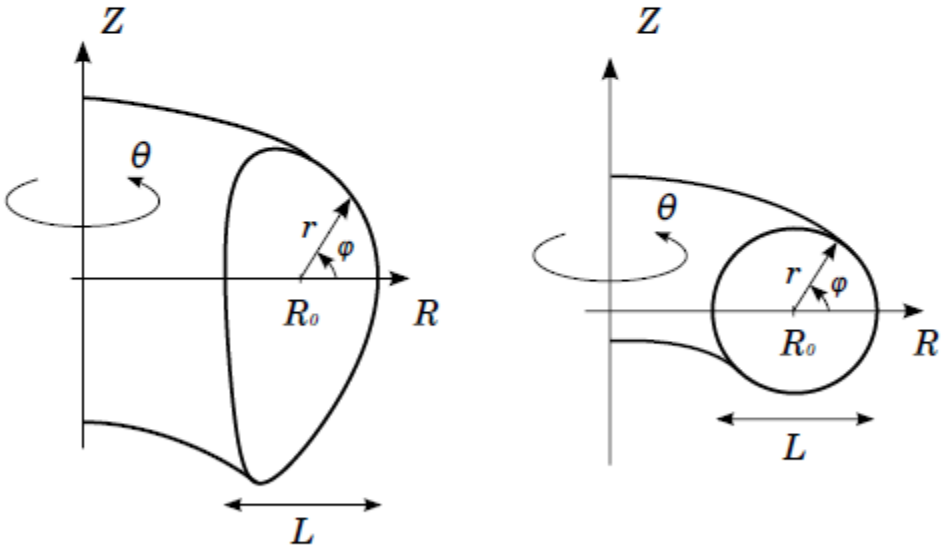


Asymmetric 'D' Circular

Figure: The toroidal direction is labelled $\theta$ and the poloidal $\varphi$.

# The volume penalization method

How do we solve the equations?

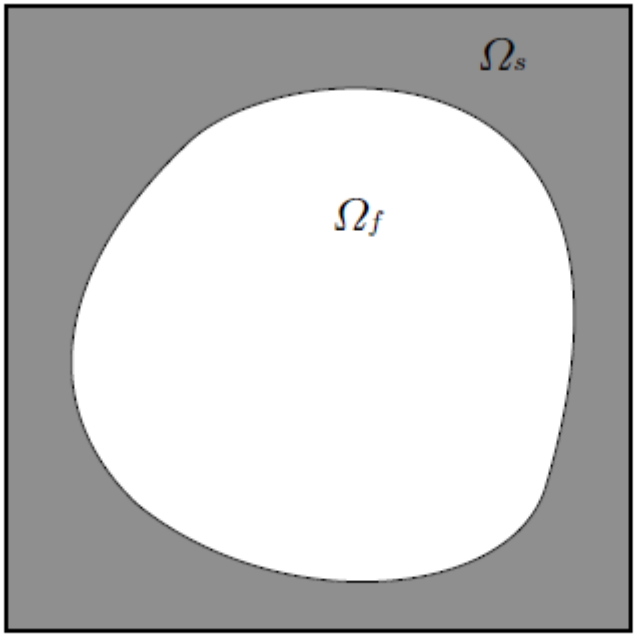


$$\chi(\boldsymbol{x},t)=\begin{cases}0 & \text{for } \boldsymbol{x}\in\Omega_f, \text{ the fluid domain}\\ 1 & \text{for } \boldsymbol{x}\in\Omega_s, \text{ the solid domain.}\end{cases}$$

The computational domain $\Omega$ contains both the fluid domain $\Omega_f$ and the solid domain $\Omega_s$.

$$\frac{\partial \boldsymbol{u}}{\partial t}=\boldsymbol{u}\times\boldsymbol{\omega}-\nabla\Pi+\nu\nabla^2\boldsymbol{u}+\boldsymbol{j}\times\boldsymbol{B}-\frac{\chi}{\eta}(\boldsymbol{u}-\boldsymbol{u}_{wall})$$

$$\frac{\partial \boldsymbol{B}}{\partial t}=\nabla\times(\boldsymbol{u}\times\boldsymbol{B})+\lambda\nabla^2\boldsymbol{B}-\frac{\chi}{\eta}(\boldsymbol{B}-\boldsymbol{B}_{wall}),$$

Fourier pseudo-spectral method with semi-implicit time stepping.

# Numerical simulations

## Symmetric geometry

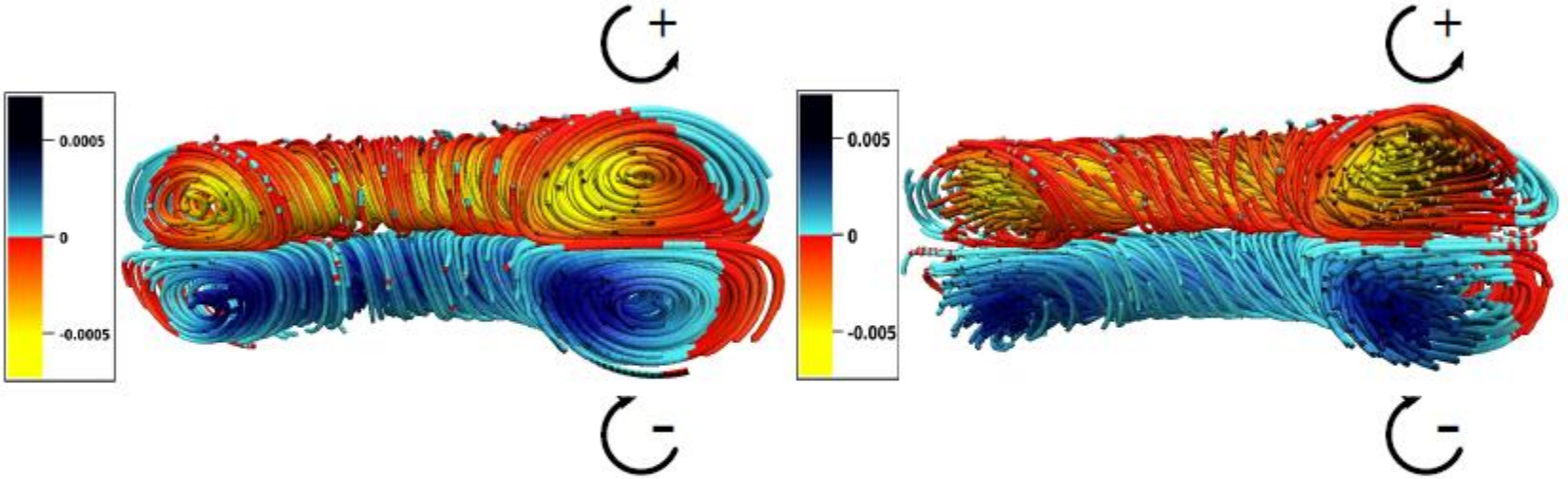


Figure: Symmetric geometry. Streamlines colored with toroidal velocity ($u_\theta$) for $M = 7.5$ (left) and $M = 75.2$ (right).

- In the limit of vanishing nonlinearity Bates & Montgomery (1998) showed analytically that the steady state solution is a pair of poloidally **counter-rotating vortices**.



Ref.: J. Morales, W. Bos, K. Schneider and D. Montgomery, *Phys. Rev. Lett.*, **109** , 2012.

# Numerical simulations

## Asymmetric geometry

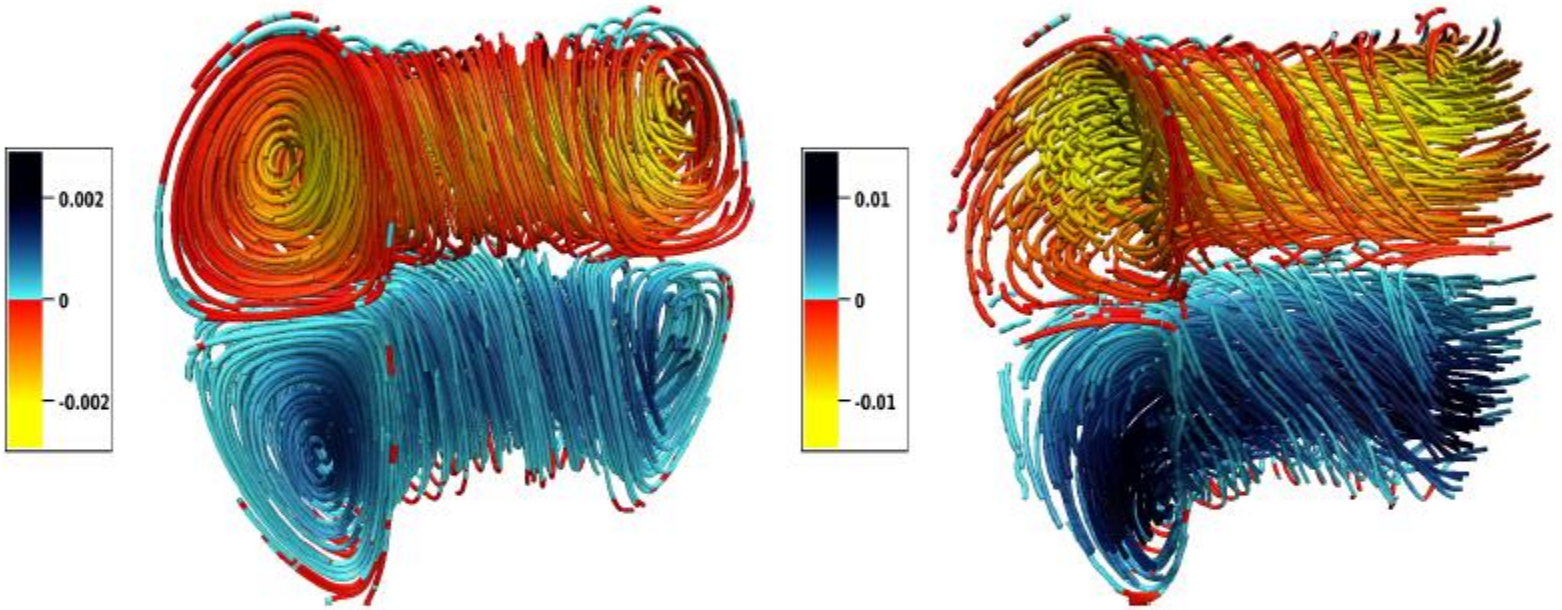


Figure: Asymmetric geometry. Streamlines colored with toroidal velocity ($u_\theta$) for $M = 7.5$ (left) and $M = 75.2$ (right).

- There is a **transition**, the spontaneously generated flow changes from dominantly poloidal to **dominantly toroidal**.



Ref.: J. Morales, W. Bos, K. Schneider and D. Montgomery, *Phys. Rev. Lett.*, **109** , 2012.

# Influence of the Lundquist number

- The **toroidal velocity increases** with the viscous Lundquist number $M$.
- For the symmetric and asymmetric geometry the volume-average square toroidal velocity saturates for increasing $M$ number to $\sim$ **86%** of the total square speed.

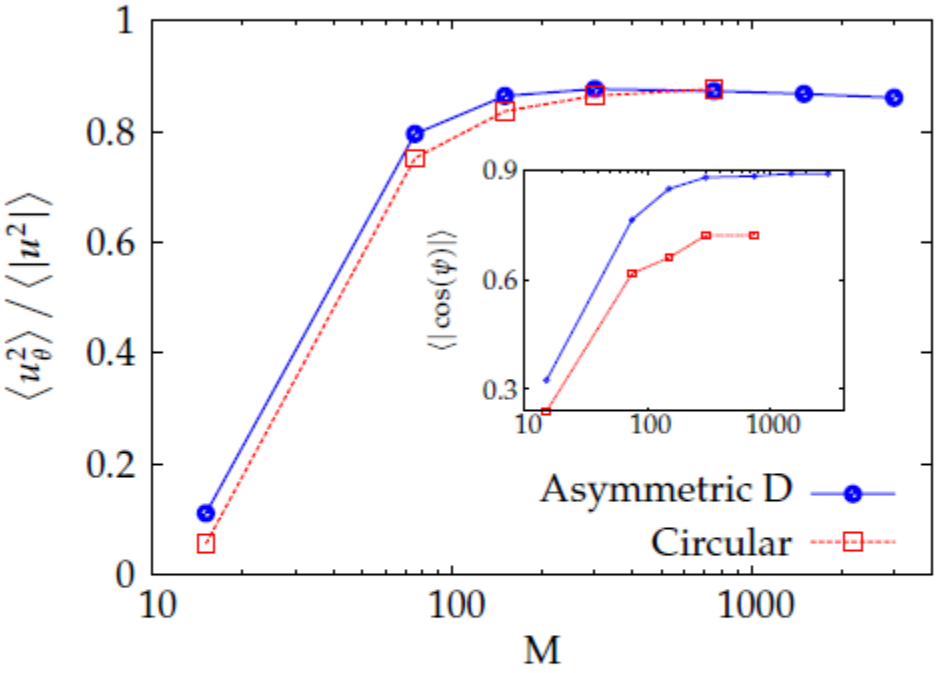


Figure: $\langle u_\theta^2 \rangle / \langle |\boldsymbol{u}^2| \rangle$ as a function of $M$.

- The toroidal organization is consistent with the tendency of the **velocity-field to align with the magnetic field** (see insert).



Ref.: J. Morales, W. Bos, K. Schneider and D. Montgomery, *Phys. Rev. Lett.*, **109** , 2012.

# Effect of an up-down asymmetry

- A fundamental **difference** is observed between the two geometries.
- For the symmetric cross section the volume averaged toroidal angular momentum is zero.

$$\langle L_\theta \rangle = \frac{1}{V} \int_V R u_\theta dV. \quad (8)$$

- For the **asymmetric** case, **toroidal angular momentum increases** with the Lundquist number.

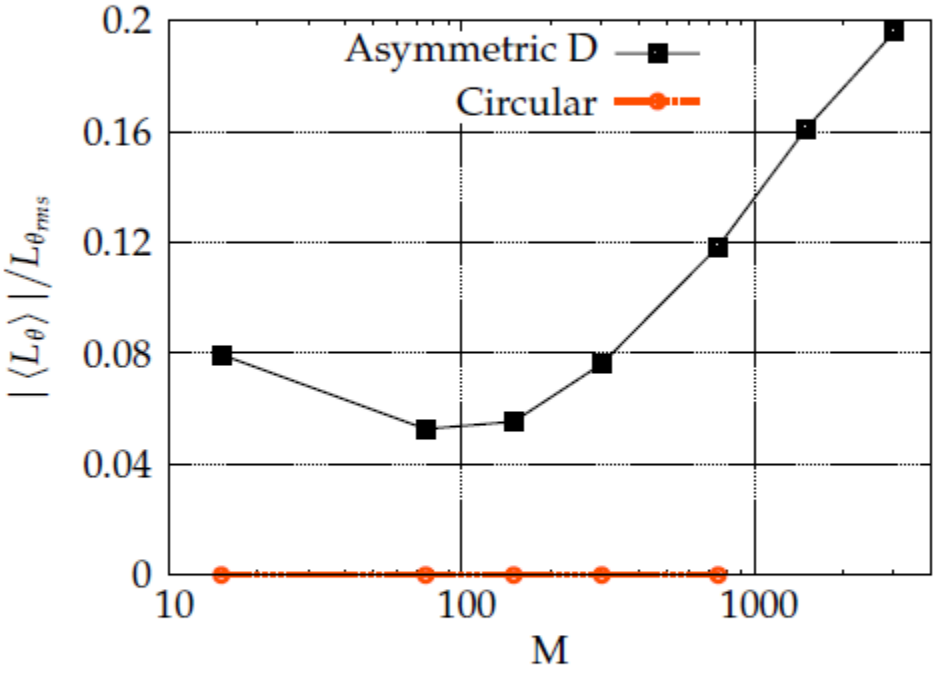


Figure: $|\langle L_\theta \rangle|/L_{\theta_{rms}}$ as a function of $M$.



Ref.: J. Morales, W. Bos, K. Schneider and D. Montgomery, *Phys. Rev. Lett.*, **109** , 2012.

# Effect of an up-down asymmetry

- Azimuthally averaged flow visualizations of the toroidal velocity $u_\theta$ and toroidal velocity profiles along a vertical cut,

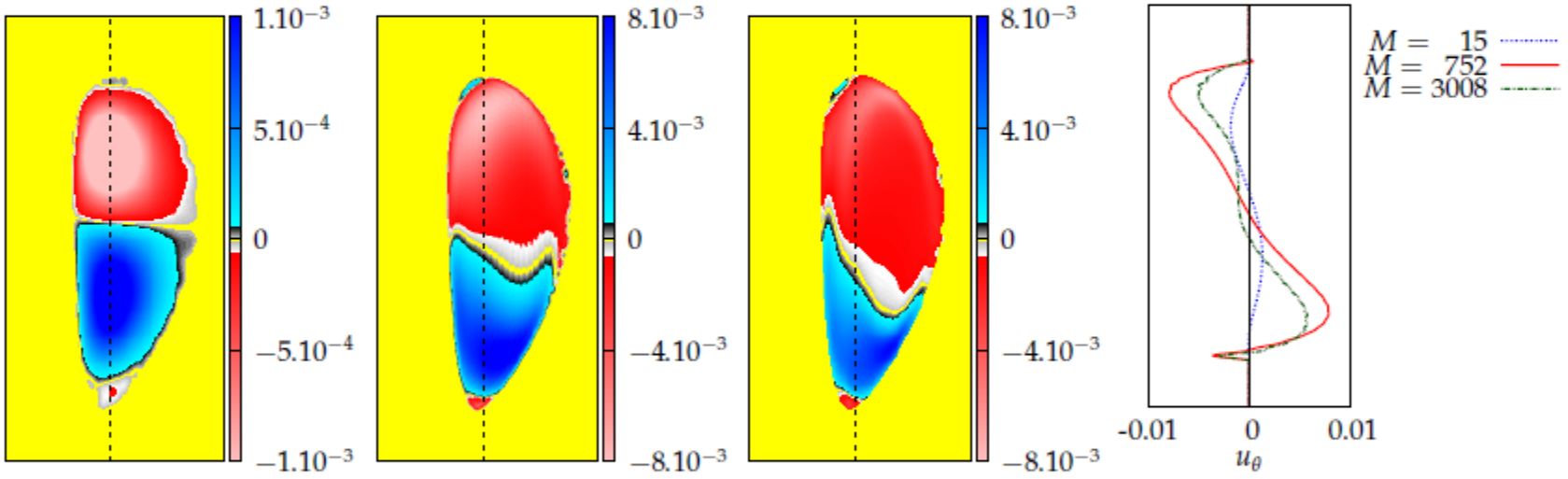


$M = 15.$ $M = 752.$ $M = 3008.$ Vertical cut.

- This **symmetry breaking** leads to the development of a net toroidal flow.



Ref.: J. Morales, W. Bos, K. Schneider and D. Montgomery, *Phys. Rev. Lett.*, **109** , 2012.

# Conclusion

- Considering **curl-free** toroidal electric and magnetic fields, **constant** transport coefficients in a **toroidal geometry** → spontaneous generation of **velocity fields**.
- This velocity field aligns (or antialigns) with the magnetic field → important **toroidal component**. This is a **nonlinear effect**.
- **Toroidal angular momentum is created if the up-down symmetry of the torus is broken**.

J.A. Morales, W.J.T. Bos, K. Schneider and D.C. Montgomery. ***Intrinsic Rotation of Toroidally Confined Magnetohydrodynamics***. Physical Review Letters, **109(17)**, 175002, (2012).

# Application to

# Effect of toroidicity in RFP dynamics

Ref.: J. Morales, W. Bos, K. Schneider and D. Montgomery, *Plasma Phys. Control. Fusion*, **56** , 2014.

# RFP in toroidal and cylinder geometry

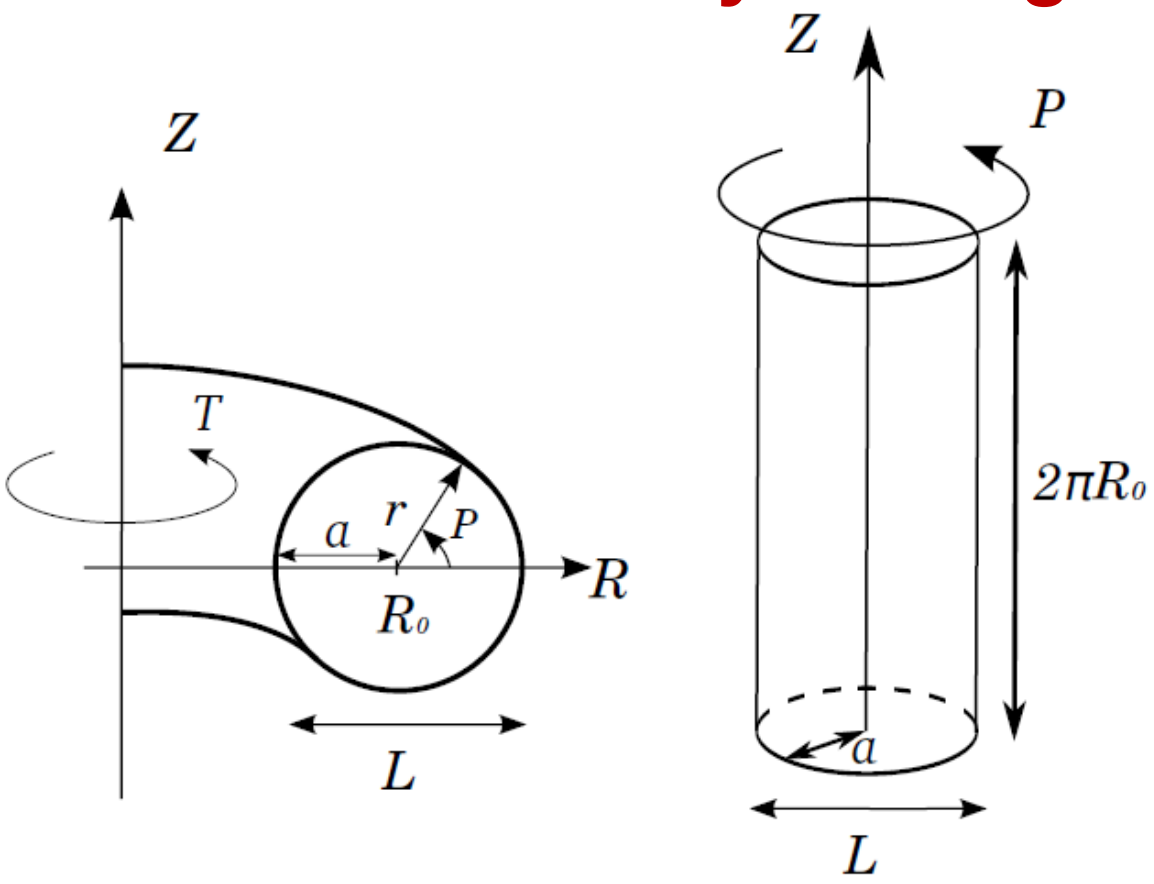


**Figure 1.** Toroidal (left) and periodic cylinder geometry (right). The toroidal direction is labeled $T$ and the poloidal $P$.

Pinch ratio $\Theta = \overline{B_P}/\langle B_T \rangle$ :
wall averaged poloidal mag. field / volume averaged toroidal mag. field

# RFP dynamics (torus)



ratio of kinetic energy of the dominant toroidal mode over tot. kin. energy

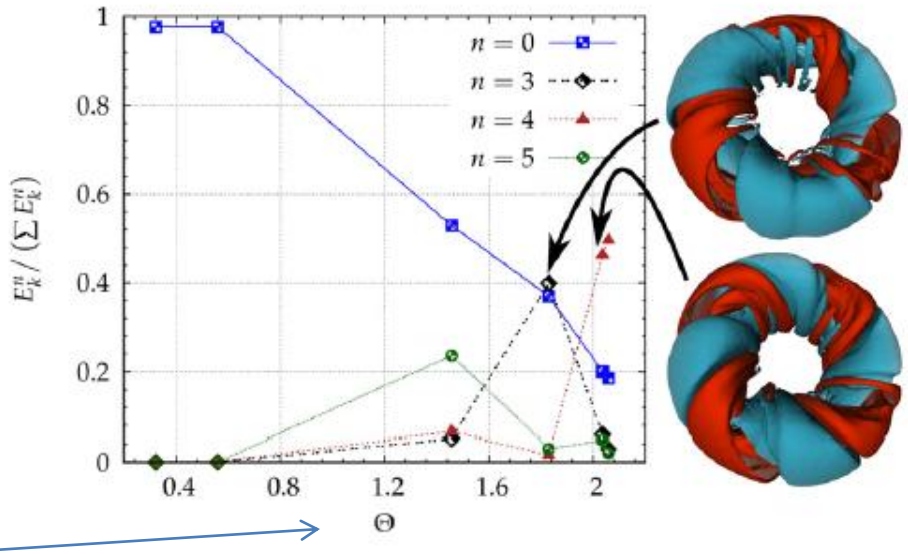


Toroidal velocity isosurfaces

pinch ratio

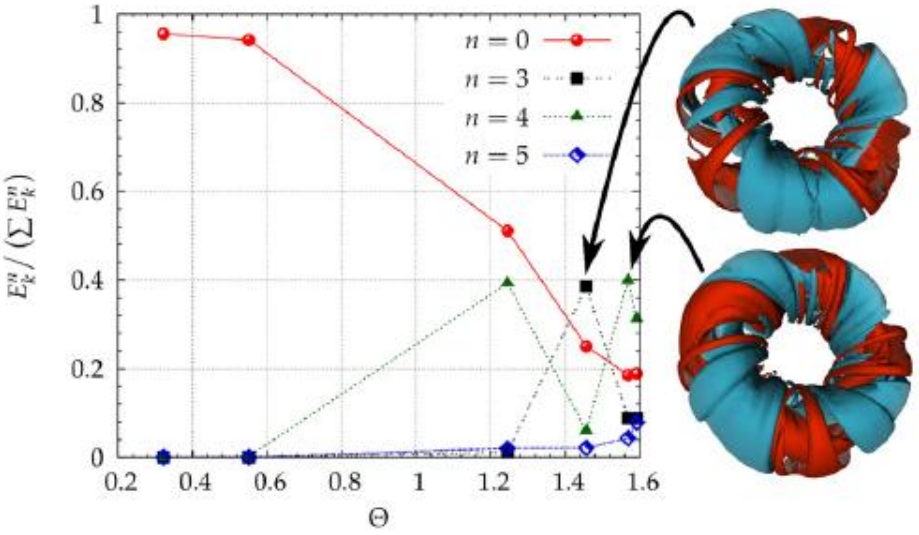


**Figure 2.** Ratio of the kinetic energy of the dominant toroidal modes over the total kinetic energy for the torus geometry, $M = 444$ (top) and $M = 888$ (bottom) as a function of $\Theta$. Visualization of the modes: toroidal velocity isosurfaces +0.007 (blue) and −0.007 (orange).

# RFP dynamics (cylinder)



ratio of kinetic energy of the dominant axial mode over tot. kin. energy

pinch ratio

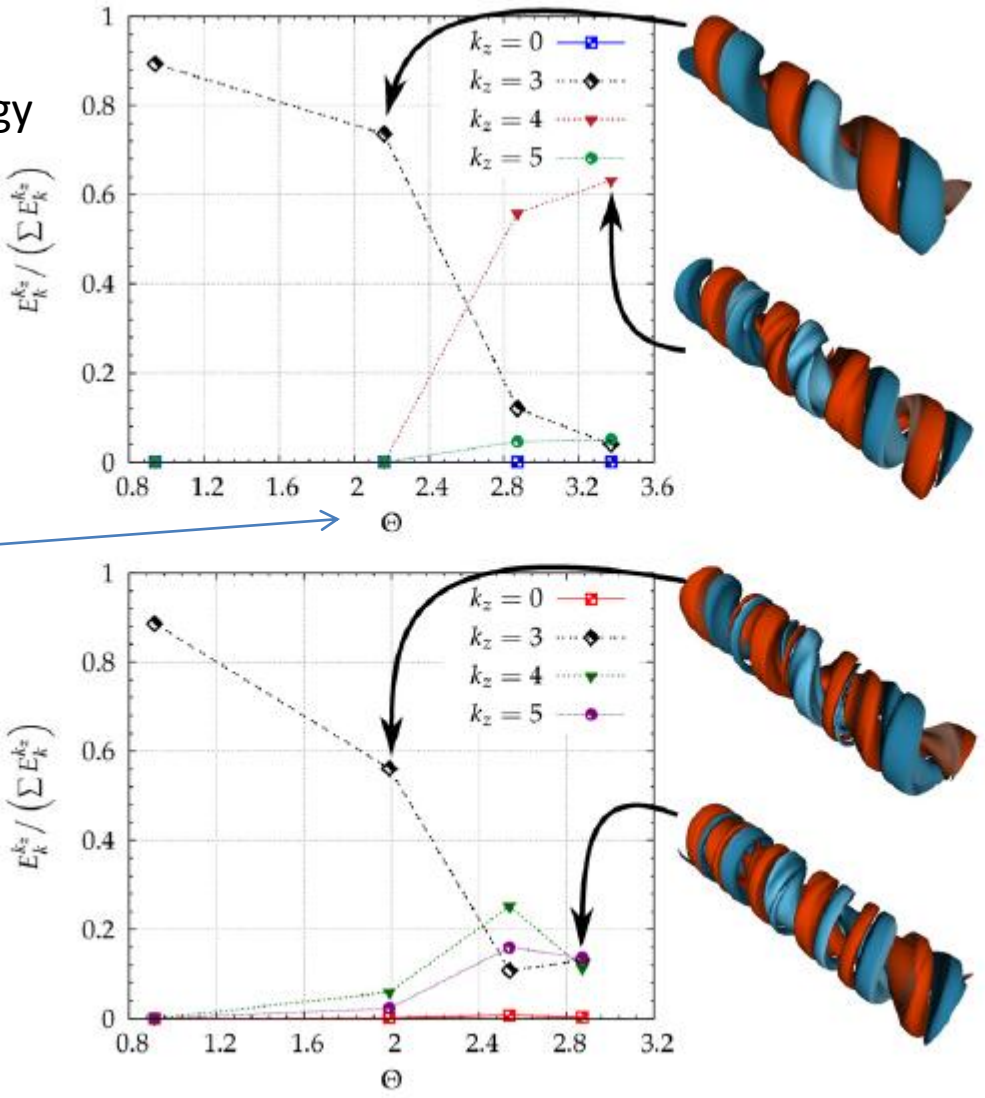


Axial velocity isosurfaces

**Figure 3.** Ratio of the kinetic energy of the dominant axial modes over the total kinetic energy for the cylindrical geometry, $M = 444$ (top) and $M = 888$ (bottom) as a function of Θ. Visualization of the modes: axial velocity isosurfaces +0.008 (blue) and −0.008 (orange).

# Conclusions: RFP dynamics

• Influence of curvature of the imposed magnetic field on Reversed Field Pinch dynamics was investigated.

• Comparison of a toroidal with a periodic cylindrical geometry.

• Axisymmetric toroidal mode is always present in the toroidal, but absent in the cylindrical configuration.

• Toroidal case presents a double poloidal recirculation cell with a shear localized at the plasma edge.

• Quasi-single-helicity states more persistent in toroidal than in the periodic cylinder .

Ref.: J. Morales, W. Bos, K. Schneider and D. Montgomery, *Plasma Phys. Control. Fusion*, **56** , 2014.

# Conclusions

- Volume penalization to model fluid and plasma flows in complex (time varying) geometries.
- Simple 1d examples for the penalized Laplace with Dirichlet or Neumann boundary conditions.
- Optimal penalization parameter $\eta_{opti}$ is of order $N^{-2}$
- The finest resolved scale should be of $O(\eta^{1/2})$
- Cancellation of penalization and discretization errors.
- Applications to 2d confined fluid turbulence, fluid-structure interaction, …
- Application to plasma turbulence:
    - Spontaneous spin-up in toroidal geometries
    - Effect of toroidicity in RFP devices.

Some Theory:

Ref.: R. Nguyen van yen, D. Kolomenskiy, K. Schneider, *Numerische Mathematik*, in press, 2014 and *Appl. Num. Math.*, in press, 2014

www.cmi.univ-mrs.fr/~kschneid

# Thank you very much for your attention!